Chemical Science

ROYAL SOCIETY OF CHEMISTRY

EDGE ARTICLE

View Article Online
View Journal | View Issue

Check for updates

Cite this: *Chem. Sci.*, 2023, **14**, 5214

All publication charges for this article have been paid for by the Royal Society of Chemistry

Received 29th March 2023
Accepted 20th April 2023

DOI: 10.1039/d3sc01635h

rsc.li/chemical-science

Insertion of CO_2 and CS_2 into Bi–N bonds enables catalyzed CH-activation and light-induced bismuthinidene transfer†

Kai Oberdorf,[a] Anna Hanft,[a] Xiulan Xie,[a] F. Matthias Bickelhaupt,[bcd] Jordi Poater *[e] and Crispin Lichtenberg *[a]

The uptake and release of small molecules continue to be challenging tasks of utmost importance in synthetic chemistry. The combination of such small molecule activation with subsequent transformations to generate unusual reactivity patterns opens up new prospects for this field of research. Here, we report the reaction of CO_2 and CS_2 with cationic bismuth(III) amides. CO_2-uptake gives isolable, but metastable compounds, which upon release of CO_2 undergo CH activation. These transformations could be transferred to the catalytic regime, which formally corresponds to a CO_2-catalyzed CH activation. The CS_2-insertion products are thermally stable, but undergo a highly selective reductive elimination under photochemical conditions to give benzothiazolethiones. The low-valent inorganic product of this reaction, Bi(I)OTf, could be trapped, showcasing the first example of light-induced bismuthinidene transfer.

Introduction

The activation of small molecules such as H_2, CO, CO_2, P_4, and ethylene used to be considered a domain of transition-metal complexes, but recent advances in main group chemistry have set the stage for s- and p-block compounds to become a unique part of this field of research.[1–8] Strategies that have successfully been applied for small molecule activation by main group compounds include the exploitation of frustrated Lewis pairs,[6] low valent species,[1–4] (bi)radicals,[1–4,9] compounds featuring element–element multiple bonds,[1–4] ring-strain,[2,10] shuttling between unusual oxidation states,[11,12] and element-ligand cooperativity.[8]

Among the main group compounds, species based on heavy p-block elements with a main quantum number ≥5 stand out due to large covalent radii, flexible coordination environments, soft Lewis acidity, relativistic effects becoming more relevant, and low bond dissociation energies.[13–17] These properties have paved the ground for fundamentally important findings, including the reversible addition of H_2 and ethylene to distannynes,[18] the reversible fixation of CO_2 and CS_2 by complexes with hyper-coordinate antimony or bismuth centers,[19,20] CO insertion into a Bi–N bond,[10] and the reversible P_4 activation by a bismuth radical.[21] The valuable insights gained from research

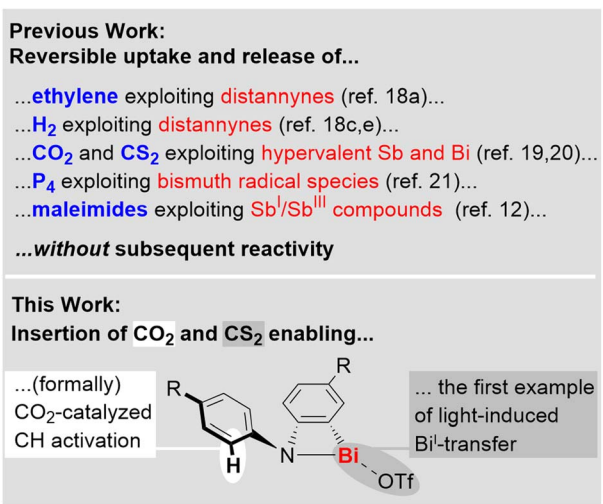

Scheme 1 Activation of small molecules with compounds of heavy p-block elements. Top: reversible activation without subsequent novel reactivity (literature). Bottom: activation of CO_2 and CS_2 followed by CH activation and light-induced bismuthinidene transfer (this work).

[a]Fachbereich Chemie, Philipps-Universität Marburg, Hans-Meerwein-Str. 4, 35043 Marburg, Germany. E-mail: crispin.lichtenberg@chemie.uni-marburg.de
[b]Theoretical Chemistry, Department of Chemistry and Pharmaceutical Sciences, Vrije Universiteit Amsterdam, The Netherlands
[c]Institute for Molecules and Materials, Radboud University, Heyendaalseweg 135, 6525 AJ Nijmegen, The Netherlands
[d]Department of Chemical Sciences, University of Johannesburg, Auckland Park, Johannesburg 2006, South Africa
[e]Departament de Química Inorgànica i Orgànica, IQTCUB, Universitat de Barcelona, ICREA, Pg. Lluís Companys 23, 08010 Barcelona, Spain. E-mail: jordi.poater@ub.edu

† Electronic supplementary information (ESI) available: Experimental details, crystallographic information; computational details; cartesian coordinates of calculated compounds. CCDC 2223276–2223278. For ESI and crystallographic data in CIF or other electronic format see DOI: https://doi.org/10.1039/d3sc01635h

in this field have so far mostly been focused on the activation, release, and degradation of small molecules, as well as their utilization as building blocks (for highlights on the reversible uptake and release of small molecules see: Scheme 1, top). In contrast, the concept of incorporating a small molecule into a heavy main group complex in order to grant access to new reactivity patterns in subsequent reactions is far less explored. This requires the generation of reactive sites that can be addressed by an external stimulus. Along these lines, the insertion of CO_2 and CS_2 into well-defined bismuth complexes is a promising approach, since Bi–O and Bi–S bonds can readily be cleaved *via* heterolytic or homolytic pathways[22–24] and even chelating bonding modes of carboxylates and dithiocarboxylates do not generate deep thermodynamic sinks due to the coordination chemical flexibility of the large central atom (Scheme 1, bottom).

Here we report the selective insertion of CO_2 and CS_2 into the Bi–N bonds of cationic bismuth amides and the unusual reactivity patterns of the resulting products, which cover CH activation and an unprecedented light-induced bismuthinidene transfer.

Results and discussion

Previously reported ring-strained cationic bismuth compounds **1-R** were selected as starting materials since they exhibit a sufficiently high reactivity and one reactive site per bismuth atom (Scheme 2a).[25–27] Reactions of **1-R** with CO_2 and CS_2 gave compounds **2-R** and **3-R** in 72–89% yield, resulting from the selective insertion of the heterocumulenes into the Bi–N bond (Scheme 2a). These are rare examples of compounds based on heavier p-block elements, for which well-defined insertion reactions with both, CO_2 and CS_2 could be realized.[28] NMR spectra of **2-R** and **3-R** revealed the expected signal patterns, albeit signal broadening was observed for **3-R** (and for **2-R** in pyridine), suggesting the accessibility of higher aggregates in equilibrium reactions. This is supported by a combination of DOSY NMR spectroscopy, high-resolution mass spectrometry, and DFT calculations. DOSY NMR spectroscopy indicated the presence of aggregated species, where the formally determined degrees of aggregation represent averaged values when involving equilibrium reactions that proceed beyond the time scale of the experiment.[29] For **2-H**, high-resolution ESI-MS revealed a mononuclear species resulting from loss of CO_2 and the $[OTf]^-$ counteranion, suggesting the possibility of de-aggregation and giving a first hint at the facile liberation of CO_2 from this molecule (*vide infra*). For **3-H** mono- and dinuclear monocations (obtained by loss of $[OTf]^-$) were detected. DFT calculations at the ZORA-BLYP-D3(BJ)/TZ2P level[30] with a pyridine solvent model, suggest that the aggregation to form a dinuclear species is energetically disfavored for **2-H** (ΔG = +10.9 kcal mol^{-1}), but feasible for **3-H** ($\Delta G = -8.8$ kcal mol^{-1}).[29] Overall, these results suggest that the solution structures of compounds **2-R** and **3-R** involve aggregation phenomena with mononuclear species being accessible. The mononuclear representation of these compounds in Scheme 2 is chosen for simplicity.

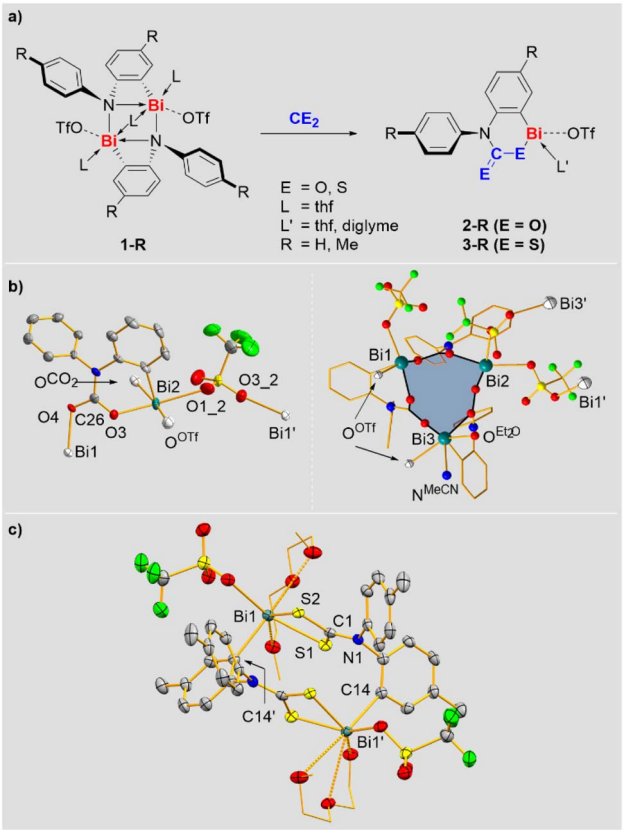

Scheme 2 (a) Insertion of CO_2 and CS_2 into Bi–N bonds to give **2-R** and **3-R**. For a discussion of the CE_2-bonding mode and the aggregation behavior of **2-R** and **3-R** see main text. A mononuclear representation of **2-H** and **3-H** is chosen for simplicity. (b and c) Molecular structures of **2-H** (b) and **3-Me** (c) in the solid state. Displacement ellipsoids are shown at the 50% probability level. Hydrogen atoms are omitted for clarity and C atoms are shown as wireframe in the right part of (b); atoms exceeding one subunit are drawn as white ellipsoids. Selected bond lengths [Å] for **2-H**: Bi1–O4, 2.232(5), Bi2–O3, 2.222(5); Bi2–C14, 2.206(8). Selected bond lengths [Å] for **3-Me**: Bi1–S1, 2.6260(8); Bi1–S2, 2.6354(7), Bi1–C14′, 2.305(3); S1–C1, 1.716(3); S2–C1, 1.720(3); C1–N1, 1.332(4).

The molecular structures of **2-R** and **3-R** in the solid state were elucidated by single-crystal X-ray diffraction analyses and evidence the coordination chemical flexibility of cationic bismuth species (the quality of the X-ray data on **2-Me** and **3-H** does not allow the discussion of bonding parameters, but serves as a proof of connectivity). Single-crystals of **2-H** were obtained by layering a saturated solution of **2-H** in acetonitrile with diethyl ether, leading to partial exchange of the solvent ligands (*vide infra*). The CO_2 moieties in **2-H** adopt bridging μ_2-η^1,η^1-coordination modes to form a trinuclear species (one mononuclear subunit and the trimer are depicted in Scheme 2b). Two of the three triflate anions also adopt a bridging coordination mode, resulting in the interconnection of trinuclear subunits to form a double-stranded coordination polymer along the crystallographic *b*-axis. The bismuth atoms Bi1 and Bi2 adopt a square pyramidal coordination geometry due to contacts with one aryl, two triflate and two CO_2 units, while Bi3 shows a very

unusual pentagonal pyramidal coordination geometry due to contacts with one aryl, one triflate, one CO_2 moiety and two neutral ligands (Et_2O and MeCN). The Bi–O bonds (2.22–2.30 Å) and the C–O bonds (1.27–1.30 Å) involving CO_2 moieties are similar in length, suggesting a delocalization of electron density across the CO_2 unit. The analysis of **2-Me** confirmed the μ_2-η^1:η^1-coordination mode of the CO_2 group and the tendency towards aggregation in the solid state (to form a dinuclear species in this case).[29]

The structural analysis of **3-R** gives further evidence of the rich coordination chemistry of bismuth cations: **3-H** forms a tetranuclear species with the CS_2 moiety in a bridging μ_2-η^1,η^1-coordination mode, while **3-Me** crystallized as a dinuclear aggregate with the CS_2 unit showing a non-bridging, chelating η^1,η^1-coordination (Scheme 2c).[29] The bismuth atoms in **3-Me** show a coordination number of seven with an irregular coordination geometry around Bi1. The Bi1–S1/2 bond lengths (2.63–2.64 Å) do not differ significantly. Together with the C1–S1/2 distances (1.72 Å), which are identical within limits of error, they indicate effective delocalization of the electron density in the CS_2 unit.

While only a few bismuth compounds have been reported to selectively react with CO_2 or CS_2, even less is known about the reactivity of the products resulting from these reactions.[19,28,31] As a prominent example, the shallow potential energy landscape related to the insertion of CO_2 into a Bi–O bond of $(Ar_2Bi)_2O$ has been exploited to reversibly bind and release this heterocumulene.[19] Inspired by these pivotal contributions, we set out to map the reactivity of **2-R** and **3-R** centered around the stimulus-induced release of CO_2 and CS_2.

Indeed, compounds **2-R** eliminate CO_2 at ambient temperature in pyridine or at 60 °C in THF, irrespective of the presence or absence of ambient light. The decay of **2-R** and the formation of CO_2 was monitored by ^{1}H and ^{13}C NMR spectroscopy, respectively. Remarkably, the CO_2 release goes along with selective formation of the previously reported[25–27] *ortho* CH-activation products **4-R** in quantitative spectroscopic yield (Scheme 3a). The formation of **4-Me** was also confirmed by single-crystal X-ray analysis.[29] Access to the *ortho* CH-activated species **4-R** has previously been achieved by heating **1-R** in pyridine at 80 °C (Scheme 3a, bottom).[25,27] When THF is used as the solvent, **1-H** in particular can be kept at 60 °C over an extended period of time without any signs of decomposition or transformation.[32] In the presence of 10 mol% of **2-H**, however, compound **1-H** was readily transformed into **4-H** with >90% spectroscopic yield over 4 days in THF (Scheme 3a, bottom). Lowering the amount of **2-H** in the reaction mixture to 1 mol% still resulted in the selective formation of **4-H** (84% spectroscopic yield), albeit longer reaction times of 17 d were necessary. These observations *formally* correspond to a CO_2-catalyzed CH-activation reaction.[33] In contrast to the CO_2-insertion products **2-R**, the sulfur analogs **3-R** proved to be stable in THF at 60 °C over days, when ambient light was excluded.

Mechanistic aspects of the CE_2 extrusion from **2-H** and **3-H** were investigated by DFT calculations (Scheme 3b). Mononuclear model systems were chosen based on the investigations of their aggregation behavior (*vide supra*), to keep the

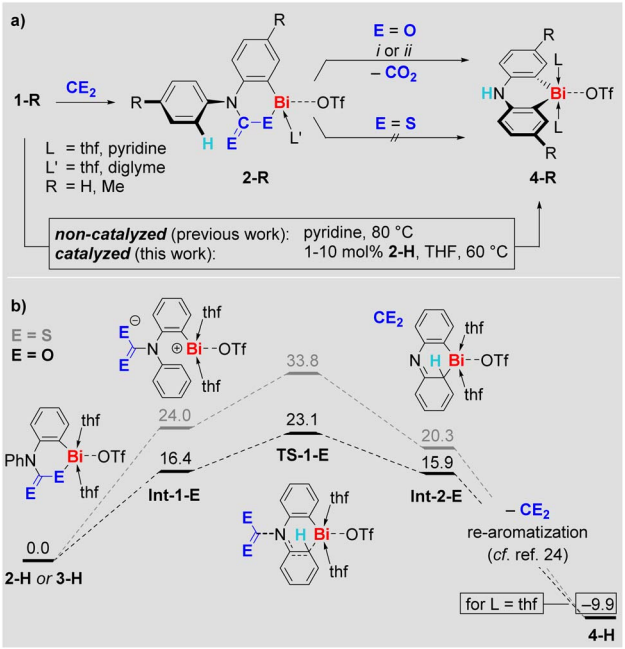

Scheme 3 (a) Reactivity of compounds **2-R** in the context of CH activation of **1-R** to give **4-R** ((i) THF, 60 °C, (ii) pyridine, r.t.). (b) Proposed mechanism for the extrusion of CE_2 from **2-H** (black) and **3-H** (dark grey) to give **4-H**. Gibbs energies are given in kcal mol^{-1}.[29]

computational approach feasible at a sufficiently high level of theory, and because a higher reactivity for mononuclear species has been proposed in related systems.[34] We suggest a heterolytic cleavage of the Bi–E bond as the initiating step of the reaction to give the charge-separated intermediate **Int-1-E**. This intermediate is energetically more favorable for E = O than for E = S due to stabilization of the negative charge by the electronegative oxygen atoms in the $(R_2NCO_2)^-$ moiety. Release of CE_2 with concomitant addition of the cationic bismuth center to the phenyl group *via* transition state **TS-1-E** gives **Int-2-E**. Again, the oxygen-based species is lower in energy, which is due to the energy gain resulting from the formation of the C=E double bond in CE_2 being higher for E = O than for E = S.[35] Re-aromatization of **Int-2-E** gives the final product **4-H** – a sequence of reactions that has previously been investigated in detail during the CH activation of **1-H** and is thus suggested to proceed in an analogous manner here.[25] Overall, the results of this mechanistic study indicate release of CO_2 at early stages of the reaction, rationalize the feasibility *vs.* reluctance of CE_2 release for **2-R** and **3-R**, and demonstrate the accessibility of previously identified reaction pathways for bismuth-mediated CH activation upon CE_2 elimination. The sensitivity of the CH activation **1-H** → **4-H** towards the polarity of the reaction medium[32] motivated us to investigate the effect of the CO_2 insertion on the polarity of the bismuth species by DFT methods. Indeed, the CO_2-insertion-product **2-H** shows a high dipole moment of 6.1 D, exceeding those of pyridine (2.3 D) or 1,2-difluorobnezene (2.6 D), which also facilitate the CH activation of **1-H** when used as solvents.[29] These findings indicate that an increase of the polarity of the solvent medium as a result

of CO_2 insertion is an important factor facilitating the CO_2-catalyzed CH activation **1-H**–(cat. **2-H**) → **4-H**.

When solutions of compounds **2-R** were irradiated with a low-pressure Hg-lamp, only mixtures of products were obtained, which could not be identified to date.[29] While compounds **3-R** are stable in the dark, even at elevated temperature (*vide supra*), it quickly became evident that they are light-sensitive: at 23 °C, exposure of THF solutions of **3-R** to ambient light induced a quantitative and highly selective transformation over five days with concomitant precipitation of a dark solid. Irradiation of THF solutions of **3-R** with a low-pressure Hg-vapor lamp dramatically accelerated these reactions without diminishing the excellent selectivities (full conversion after 45 min).[29] The THF-soluble products of these reactions were identified as benzothiazolethiones **5-R** (Scheme 4, top). This corresponds to a C–S bond formation, formally resulting from the reductive elimination of $Bi^{I}(OTf)$, which we suggest as a logical intermediate. DFT calculations confirm that a concerted mechanism only involving closed-shell species is too high in energy to be viable.[29] In contrast, DFT calculations suggest that the light-induced Bi–S homolysis in **3-R** is feasible and gives a short-lived intermediate (**Int-5-S**; ESI†), from which the elimination of $Bi(thf)_2(OTf)$ proceeds with a free activation energy of only 9.0 kcal mol^{-1}.[29] It should be noted in this context that $Bi^{I}(OTf)$ has recently been isolated as a cyclic alkyl(amino) carbene adduct and proved to be unstable in solution.[36] In general, non-stabilized bismuthinidenes BiX (X = monoanionic, monodentate ligand) are unstable in solution,[16,37] with disproportionations such as 3 BiX → 2 Bi^0 + BiX_3 being a typical degradation pathway, which accounts for the commonly observed dark precipitate ("bismuth black").[38] In order to trap the potential intermediate $Bi^{I}(OTf)$ in photochemical reactions of cationic bismuth species, 3,5-di-*tert*-butyl-*o*-benzoquinone (**6**) was added to a THF solution of **3-H**. ^{1}H NMR spectroscopy revealed that the quinone coordinated **3-H**, but no reaction occurred at ambient temperature in the dark. Upon irradiation of the reaction mixture containing the quinone (Scheme 4, bottom), the precipitation of a black solid was not observed and quantitative conversion to **5-H** and a new compound (later identified as **7**) was detected by NMR spectroscopy. Despite similar solubilities of these two products, compound **7** could be isolated in moderate yield and was fully characterized.[29]

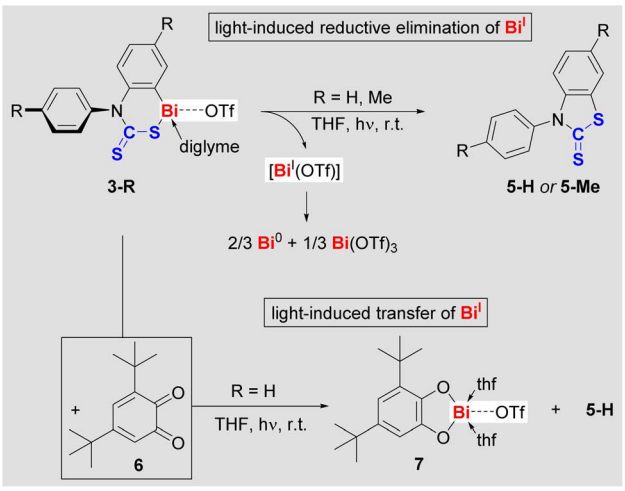

Scheme 4 Photochemically-induced elimination of BiOTf from **3-R** to give heterocycle **5-R** in the absence (top) and presence (bottom) of 3,5-di-*tert*-butyl-*o*-benzoquinone (**6**), which is introduced as bismuthinidene trapping reagent.

While the chemistry of mononuclear bismuth compounds used to be centered around Bi^{III} and Bi^{V} species, recent advances have begun to uncover an unexpectedly rich redox chemistry for this class of compounds.[7,11,14,39] This includes examples of reductive elimination reactions for selective bond formation in stoichiometric or catalytic regimes, which operate under thermal conditions.[15,40] While the light-sensitivity of molecular bismuth compounds has been phenomenologically described,[41] the exploitation of their photochemistry for selective bond formations is still in its infancy.[23,24] Similarly, the field of cationic bismuth(I) compounds is virtually unexplored, with a single example of an isolable species[36] and the reactivity of these species being entirely unknown.[17,42] Along these lines, reactions of compounds **3-R** demonstrate for the first time that cationic bismuth compounds may be exploited both, for the light-driven construction of organic heterocycles and for photochemically-induced transfer of low-valent Bi(I) building blocks.

Conclusions

In summary we have shown, that ring-strained bismuth amide cations selectively insert CO_2 and CS_2. The insertion products show striking differences in their reactivity: the CO_2 activation products undergo thermochemical CO_2 elimination, which goes along with a CH activation to furnish previously reported cationic bisma-cycles. These reactions were transferred to the catalytic regime, which formally corresponds to an unprecedented CO_2-catalyzed CH activation reaction. In the case of the CS_2 activation product, the highly selective, photochemical elimination of low-valent BiOTf (a so-called bismuthinidene) is observed, while benzothiazolethiones are generated through selective C–S bond formation. Chemical trapping of the photochemically released BiOTf was realized for the first time, opening up the field of light-driven bismuthinidene transfer reactions, which are subject of future investigations in our laboratories.

Data availability

Experimental data is provided in the ESI.†

Author contributions

Synthesis: K. O. (exclusively); X-ray diffraction analyses: K. O., A. H. (equal); DFT calculations: J. P. (lead); F. M. B., C. L. (supporting); DOSY studies: X. X. (lead); K. O., C. L. (supporting) composition of the manuscript: K. O., C. L. (lead); J. P. (supporting); discussion of results and correction of manuscript: all

authors; project administration: C. L. (lead); acquisition of funding: K. O., J. P., F. M. B., C. L.

Conflicts of interest

There are no conflicts to declare.

Acknowledgements

We thank Benedikt Ritschel for his contributions. Financial support by the FCI, the DFG (LI2860/3-1, LI2860/5-1), the LOEWE Program, the Cusanuswerk, the Netherlands Organisation of Scientific Research (NWO), and the Spanish Government (PID-2019-106830GB-I00, CEX2021-001202-M), and the Catalan Government (2021SGR442) is gratefully acknowledged. This project has received funding from the European Research Council (ERC) under the European Union's Horizon 2020 research and innovation program (grant agreement No. 946184).

Notes and references

1 P. P. Power, *Nature*, 2010, **463**, 171–177.
2 M.-A. Légaré, C. Pranckevicius and H. Braunschweig, *Chem. Rev.*, 2019, **119**, 8231–8261.
3 C. Weetman and S. Inoue, *ChemCatChem*, 2018, **10**, 4213–4228.
4 P. P. Power, *Chem. Rev.*, 2003, **103**, 789–810.
5 D. Martin, M. Soleilhavoup and G. Bertrand, *Chem. Sci.*, 2011, **2**, 389–399.
6 D. W. Stephan, *J. Am. Chem. Soc.*, 2015, **137**, 10018–10032.
7 C. Lichtenberg, *Angew. Chem., Int. Ed.*, 2016, **55**, 484–486.
8 L. Greb, F. Ebner, Y. Ginzburg and L. M. Sigmund, *Eur. J. Inorg. Chem.*, 2020, **2020**, 3030–3047.
9 X. Yang, E. J. Reijerse, K. Bhattacharyya, M. Leutzsch, M. Kochius, N. Nöthling, J. Busch, A. Schnegg, A. A. Auer and J. Cornella, *J. Am. Chem. Soc.*, 2022, **144**, 16535–16544.
10 J. Ramler, J. Poater, F. Hirsch, B. Ritschel, I. Fischer, F. M. Bickelhaupt and C. Lichtenberg, *Chem. Sci.*, 2019, **10**, 4169–4176.
11 H. W. Moon and J. Cornella, *ACS Catal.*, 2022, **12**, 1382–1393.
12 M. Kořenková, M. Hejda, M. Erben, R. Jirásko, R. Jambor, A. Růžička, E. Rychagova, S. Ketkov and L. Dostál, *Chem.–Eur. J.*, 2019, **25**, 12884–12888.
13 (*a*) R. J. F. Berger, D. Rettenwander, S. Spirk, C. Wolf, M. Patzschke, M. Ertl, U. Monkowius and N. W. Mitzel, *Phys. Chem. Chem. Phys.*, 2012, **14**, 15520–15524; (*b*) S. Ishida, F. Hirakawa, K. Furukawa, K. Yoza and T. Iwamoto, *Angew. Chem., Int. Ed.*, 2014, **53**, 11172–11176; (*c*) T. Y. Lai, L. Tao, R. D. Britt and P. P. Power, *J. Am. Chem. Soc.*, 2019, **141**, 12527–12530; (*d*) J. Ramler and C. Lichtenberg, *Chem.–Eur. J.*, 2020, **26**, 10250–10258; (*e*) D. Dakternieks, D. J. Henry and C. H. Schiesser, *Organometallics*, 1998, **17**, 1079–1084; (*f*) J. Ramler, F. Fantuzzi, F. Geist, A. Hanft, H. Braunschweig, B. Engels and C. Lichtenberg, *Angew. Chem., Int. Ed.*, 2021, **60**, 24388–24394; (*g*) L. D. Freedman and G. O. Doak, *Chem. Rev.*, 1982, **82**, 15–57; (*h*) G. P. Smith and R. Patrick, *Int. J. Chem. Kinet.*, 1983, **15**, 167–185.
14 C. Lichtenberg, *Chem. Commun.*, 2021, **57**, 4483–4495.
15 K. Oberdorf, A. Hanft, J. Ramler, I. Krummenacher, F. M. Bickelhaupt, J. Poater and C. Lichtenberg, *Angew. Chem., Int. Ed.*, 2021, **60**, 6441–6445.
16 D. P. Mukhopadhyay, D. Schleier, S. Wirsing, J. Ramler, D. Kaiser, E. Reusch, P. Hemberger, T. Preitschopf, I. Krummenacher, B. Engels, I. Fischer and C. Lichtenberg, *Chem. Sci.*, 2020, **11**, 7562–7568.
17 J. Heine, B. Peerless, S. Dehnen and C. Lichtenberg, *Angew. Chem., Int. Ed.*, 2023, e202218771.
18 (*a*) Y. Peng, B. D. Ellis, X. Wang, J. C. Fettinger and P. P. Power, *Science*, 2009, **325**, 1668–1670; (*b*) T. Y. Lai, J.-D. Guo, J. C. Fettinger, S. Nagase and P. P. Power, *Chem. Commun.*, 2019, **55**, 405–407; (*c*) Y. Peng, M. Brynda, B. D. Ellis, J. C. Fettinger, E. Rivard and P. P. Power, *Chem. Commun.*, 2008, 6042–6044; (*d*) Y. Peng, B. D. Ellis, X. Wang and P. P. Power, *J. Am. Chem. Soc.*, 2008, **130**, 12268–12269; (*e*) S. Wang, T. J. Sherbow, L. A. Berben and P. P. Power, *J. Am. Chem. Soc.*, 2018, **140**, 590–593.
19 S.-F. Yin, J. Maruyama, T. Yamashita and S. Shimada, *Angew. Chem., Int. Ed.*, 2008, **47**, 6590–6593.
20 (*a*) L. Dostál, R. Jambor, A. Růžička, R. Jirásko, E. Černošková, L. Beneš and F. de Proft, *Organometallics*, 2010, **29**, 4486–4490; (*b*) L. Dostál, R. Jambor, A. Růžička, M. Erben, R. Jirásko, E. Černošková and J. Holeček, *Organometallics*, 2009, **28**, 2633–2636; (*c*) G. Strîmb, A. Pöllnitz, C. I. Raț and C. Silvestru, *Dalton Trans.*, 2015, **44**, 9927–9942.
21 R. J. Schwamm, M. Lein, M. P. Coles and C. M. Fitchett, *Angew. Chem., Int. Ed.*, 2016, **55**, 14798–14801.
22 (*a*) T. A. Hanna, A. L. Rieger, P. H. Rieger and X. Wang, *Inorg. Chem.*, 2002, **41**, 3590–3592; (*b*) S. Roggan, C. Limberg, B. Ziemer and M. Brandt, *Angew. Chem., Int. Ed.*, 2004, **43**, 2846–2849; (*c*) C. Limberg, *Angew. Chem., Int. Ed.*, 2003, **42**, 5932–5954.
23 J. Ramler, I. Krummenacher and C. Lichtenberg, *Chem.–Eur. J.*, 2020, **26**, 14551–14555.
24 J. Ramler, J. Schwarzmann, A. Stoy and C. Lichtenberg, *Eur. J. Inorg. Chem.*, 2022, **2022**, e202100934.
25 B. Ritschel, J. Poater, H. Dengel, F. M. Bickelhaupt and C. Lichtenberg, *Angew. Chem., Int. Ed.*, 2018, **57**, 3825–3829.
26 B. Ritschel and C. Lichtenberg, *Synlett*, 2018, **29**, 2213–2217.
27 K. Oberdorf, P. Grenzer, N. Wieprecht, J. Ramler, A. Hanft, A. Rempel, A. Stoy, K. Radacki and C. Lichtenberg, *Inorg. Chem.*, 2021, **60**, 19086–19097.
28 F. Ando, T. Hayashi, K. Ohashi and J. Koketsu, *J. Inorg. Nucl. Chem.*, 1975, **37**, 2011–2013.
29 For details see the ESI.†
30 G. te Velde, F. M. Bickelhaupt, E. J. Baerends, C. Fonseca Guerra, S. J. A. van Gisbergen, J. G. Snijders and T. Ziegler, *J. Comput. Chem.*, 2001, **22**, 931–967.
31 (*a*) S. D. Cosham, M. S. Hill, G. A. Horley, A. L. Johnson, L. Jordan, K. C. Molloy and D. C. Stanton, *Inorg. Chem.*, 2014, **53**, 503–511; (*b*) D. R. Kindra, I. J. Casely, M. E. Fieser, J. W. Ziller, F. Furche and W. J. Evans, *J. Am.*

Chem. Soc., 2013, **135**, 7777–7787; (*c*) S.-F. Yin and S. Shimada, *Chem. Commun.*, 2009, 1136–1138; (*d*) Y. Chen, R. Qiu, X. Xu, C.-T. Au and S.-F. Yin, *RSC Adv.*, 2014, **4**, 11907–11918; (*e*) K. Marczenko and S. Chitnis, *ChemRxiv*, 2021, preprint, DOI: 10.26434/chemrxiv.13619180.v2. This work has not been subjected to peer review.

32 The polarity of the reaction medium appears to be crucial for the transformation of **1-H** to **4-H**. **1-H** is stable in dichloromethane (dipole moment = 1.6 D) at 60 °C (bath temperature) for at least 3 d and in THF (dipole moment = 1.8 D) at 60 °C for at least 4 d. However, **1-H** is transformed into **4-H** in quantitative spectroscopic yield, when heated to 80 °C for 16 h in pyridine (dipole moment = 2.3 D) or 1,2-difluorobenzene (dipole moment = 2.6 D).

33 (*a*) Y. Sugawara, W. Yamada, S. Yoshida, T. Ikeno and T. Yamada, *J. Am. Chem. Soc.*, 2007, **129**, 12902–12903; (*b*) D. Riemer, B. Mandaviya, W. Schilling, A. C. Götz, T. Kühl, M. Finger and S. Das, *ACS Catal.*, 2018, **8**, 3030–3034.

34 K. Oberdorf, P. Pfister, P. Grenzer, J. Ramler, A. Hanft, A. Stoy, X. Xie and C. Lichtenberg, *Organometallics*, 2023, accepted.

35 K. B. Wiberg and Y. Wang, *Arkivoc*, 2011, **2011**, 45–56.

36 M. M. Siddiqui, S. K. Sarkar, M. Nazish, M. Morganti, C. Köhler, J. Cai, L. Zhao, R. Herbst-Irmer, D. Stalke, G. Frenking and H. W. Roesky, *J. Am. Chem. Soc.*, 2021, **143**, 1301–1306.

37 (*a*) E. H. Fink, K. D. Setzer, D. A. Ramsay and M. Vervloet, *Chem. Phys. Lett.*, 1991, **179**, 95–102; (*b*) E. Fink, K. Setzer, D. Ramsay, M. Vervloet and J. Brown, *J. Mol. Spectrosc.*, 1990, **142**, 108–116.

38 J. Bresien, A. Schulz, M. Thomas and A. Villinger, *Eur. J. Inorg. Chem.*, 2019, **2019**, 1279–1287.

39 (*a*) C. Lichtenberg, *Chem.–Eur. J.*, 2020, **26**, 9674–9687; (*b*) C. Helling and S. Schulz, *Eur. J. Inorg. Chem.*, 2020, **2020**, 3209–3221; (*c*) C. Lichtenberg, *Radical Compounds of Antimony and Bismuth in EIBC*, ed. R. A. Scott, Wiley VCH, 2020, pp. 1–12.

40 (*a*) F. Wang, O. Planas and J. Cornella, *J. Am. Chem. Soc.*, 2019, **141**, 4235–4240; (*b*) Y. Pang, M. Leutzsch, N. Nöthling and J. Cornella, *J. Am. Chem. Soc.*, 2020, **142**, 19473–19479; (*c*) Y. Pang, M. Leutzsch, N. Nöthling, F. Katzenburg and J. Cornella, *J. Am. Chem. Soc.*, 2021, **143**, 12487–12493; (*d*) W.-C. Xiao, Y.-W. Tao and G.-G. Luo, *Int. J. Hydrogen Energy*, 2020, **45**, 8177–8185; (*e*) O. Planas, F. Wang, M. Leutzsch and J. Cornella, *Science*, 2020, **367**, 313–317; (*f*) D. H. R. Barton, W. B. Motherwell and A. Stobie, *J. Chem. Soc., Chem. Commun.*, 1981, 1232–1233; (*g*) S. M. Nabavizadeh, F. Niroomand Hosseini, N. Nejabat and Z. Parsa, *Inorg. Chem.*, 2013, **52**, 13480–13489.

41 (*a*) C. Lichtenberg, F. Pan, T. P. Spaniol, U. Englert and J. Okuda, *Angew. Chem., Int. Ed.*, 2012, **51**, 13011–13015; (*b*) A. J. Ashe, E. G. Ludwig and J. Oleksyszyn, *Organometallics*, 1983, **2**, 1859–1866; (*c*) J. Lorberth, W. Massa, S. Wocadlo, I. Sarraje, S.-H. Shin and X.-W. Li, *J. Organomet. Chem.*, 1995, **485**, 149–152; (*d*) W. Clegg, N. A. Compton, R. J. Errington, G. A. Fisher, M. E. Green, D. C. R. Hockless and N. C. Norman, *Inorg. Chem.*, 1991, **30**, 4680–4682; (*e*) J. M. Wallis, G. Müller and H. Schmidbaur, *J. Organomet. Chem.*, 1987, **325**, 159–168.

42 R. Deb, P. Balakrishna and M. Majumdar, *Chem.–Asian J.*, 2022, **17**, e202101133.